Original Research Paper

Volume : 5 | Issue : 12 | December-2016 • ISSN No 2277 - 8179 | IF : 3.508 | IC Value : 78.46

STUDY OF P-E HYSTERESIS LOOPS & ELECTRICAL PROPERTIES OF LEAD FREE CERAMIC SUBSTANCE Bi0.5Na0.5Ti1-xZrxO3 [BNTZ]

Physics

KEYWORDS: Ceramics; XRD; LF- Lead free; Dielectric properties; Ferroelectricity.

ALOKE VERMA

Asstt. Professor, Department of Physics,M Kalinga University, New Raipur, (C.G.), India Pin: 492101

ABSTRACT

In this work, study of P-E hysteresis loops and electrical properties of lead-free ceramic substances BNTZ. Lead-free bismuth sodium titanate zirconate (Bi0.5Na0.5Ti1-xZrxO3) ceramics were successfully prepared using the conventional mixed-oxide method. The samples were sintered for 2 hrs at temperatures < 1,000°C. The density of the BNTZ samples was at least 95% of the theoretical values. The scanning electron microscopy micrographs showed that small grains were embedded between large grains, causing a relatively wide grain size distribution. The density and grain size increased with increasing Zr concentration. A peak shift in X-ray diffraction patterns as well as the disappearance of several hkl reflections indicated some significant crystal-structure changes in these materials. Preliminary crystal-structure analysis indicated the existence of phase transition from a rhombohedral to an orthorhombic structure. The dielectric and ferroelectric properties were also found to correlate well with the observed phase transition.

Introduction

Lead-based PT-PZ solid solutions have dominated the market of actuator and sensor materials due to their excellent ferroelectric and piezoelectric properties. In particular, a compositional ratio of Zr/Ti of around 52/48 showed the morphotropic phase boundary between a tetragonal and a rhombohedral phase, where enhanced polarizability and optimum domain orientation were observed. Therefore, researchers have attempted to develop new lead-free smart materials in order to replace the lead-based ones. BaTiO3 is one example of the most commonly used LF material for capacitors and actuators due to its inherent ferroelectric nature. However, its main disadvantage is the narrow working temperature; therefore, the use of a BT-BZ solid solution with the addition of Zr up to 30% mole was investigated. The materials were found to exhibit a composition-induced phase transition from normal to relaxor ferroelectric with a higher dielectric constant than both PZT and BT. This allowed the materials to be used over a broader temperature range. Following these studies, this paper was aimed to study BNTZ solid solutions with the addition of a Zr concentration from 0.20, 0.35, 0.40, 0.45, 0.60, and 0.80 mole fractions.

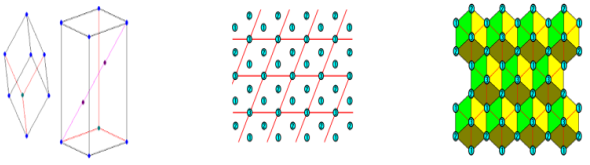

Fig.1. Rhombohedral crystal structure

Experimental Methods

For the study of ceramics substance using XRD and Mixed-Oxied method. BNTZ compositions were prepared using the mixed-oxide method incorporating Bi2O3 (> 98%), Na2CO3 (99.5%), TiO2 (> 99%,) and ZrO2 (> 99%) in stoichiometric proportions. The mixed powders were ball milled in ethanol for 24 hrs using zirconia milling media and calcined at 800°C for 2 hrs. The calcined BNTZ powders were then ball milled again for 6 hrs and uniaxially pressed at a pressure of 5.5 MPa with a few drops of 3 wt.% polyvinyl alcohol to bind it into disks of 10-mm diameter and 1.0 to 1.5-mm thickness. The disks were the sintered at 900°C for 2 hrs, except for the sample with 0.20 mole fraction Zr which was sintered at 950°C for 2 hrs, in air. The bulk densities of the sintered ceramics were measured using Archimedes' method. The theoretical density was approximated from the unit cell size and its constituent ions. Scanning electron microscopy was used to observe the microstructure of the ceramics. To prepare the SEM samples, they were well-polished and thermally etched for 15 min at 750°C. The average grain size was then evaluated from these SEM images. The room temperature dielectric constant [r] and dielectric loss [tan] were measured with an LCR meter but the ferroelectric hysteresis loops were measured in a silicone oil bath using a modified Sawyer-Tower circuit.

Results and discussion

XRD patterns of BNTZ ceramics where x = 0.20, 0.35, 0.40, 0.45, 0.60, and 0.80 mole fraction are shown in Figure 3. The BNTZ phase could be matched with pure BNT for the rhombohedral space group R3c. With the presence of Zr, all reflection peaks systematically shifted to angles lower than 2 ·. This observation suggested that the Zr4+-ion substitution into the Ti4+ site led to an enlargement of the unit cell which corresponded to the fact that the ionic radius of Zr4+ (= 0.72 Å) was larger than that of Ti4+ (= 0.605 Å). Accompanying the shift, intensities of some diffraction peaks such as (012) and (202) were reduced, indicating that lattice distortion alongside unit cell expansion has occurred. The refinement of the XRD.

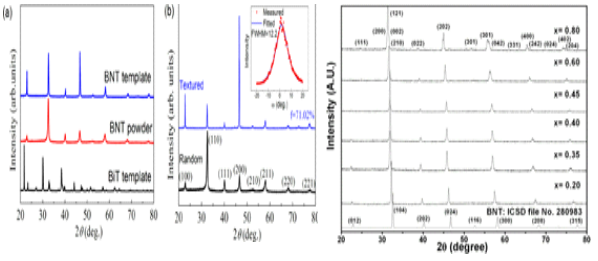

Fig.2. XRD patterns of (a) BiT template, BNT powders, BNT template, and (b) sintered randomly oriented and textured ceramics BNT–BT–3AN ceramics. Inset is the rocking curve of (2 0 0) peak of textured samples and $Bi_{0.5}Na_{0.5}Ti_{1-x}Zr_xO_3$ ceramics. Where x = 0.20, 0.35, 0.40, 0.45, 0.60, and 0.80 mole fraction.

Table 1. The refined patterns for the Zr compositions equal to 0.2 and 0.8 are also shown in Figure 5. From these data, BNTZ ceramics containing Zr from 0.2 to 0.6 possessed a rhombohedral structure with increased lattice parameters. The increase in the value of the interaxial angle caused the structure to be close to cubic, which resulted in the disappearance of certain reflections. For Zr = 0.8, Figures 1 and 3 showed an apparent splitting of the (104) and (300) peaks in the original rhombohedral structure. Based on refinement results, the structure was orthorhombic having the lattice parameters shown in Table 1. This finding was somewhat in partial agreement with the orthorhombic structure previously obtained for Bi0.5Na0.5ZrO3. Hence, for this BNTZ solid solution ceramic system, the structure changed from rhombohe dral to orthorhombic when the Zr concentration exceeded 0.6 mole fraction. The exact phase-transition composition is currently being investigated

All BNTZ ceramics had experimental density values in the range of 5.8 to 6.1 g/cm3 as shown in Table 1 which corresponded to the relative densities of around 95% of the theoretical densities. For the 0.20 mole fraction of Zr, the sample was sintered at 950°C for 2 h due to the influence of a high Ti concentration. As the amount of Zr increased, the sintering temperature could be lowered to 900°C. This

seemed to be a typical behavior of solid solutions whose melting points might be lowered by adding Zr as a deducted form of the lattice expansion. The difference in sintering behavior could also be observed from the microstructure of BNTZ ceramics; all samples were dense with well-defined grains (Figure 5). The ceramic containing Zr = 0.2 possessed an average grain size of about 0.8 μm, whereas the presence of Zr ions generally caused the grain size to increase. The enhanced ability for ionic diffusion in BNTZ ceramics seemed to support the possible lowering of the melting point of these solid solutions. The r and tan of Bi0.5Na0.5Ti1-xZrxO3 ceramics, at the frequency of 100 kHz, are tabulated in Table 1. In general, increasing Zr concentration in BNTZ ceramics caused a gradual decrease in dielectric constant with a slight decrease in dielectric loss. This behavior was in agreement with other systems with isovalent additives.

Table.1. Relation between Crystal structure and electrical properties of BNTZ ceramics

$Bi_{0.5}Na_{0.5}Ti_{1-x}Zr_xO_3$ (mole fraction)	Lattice parameter/dist ortions	Relative density	Dielectric constant (ε_r) at 100 kHz	tan	
	a, b, c (Å)		α (°)		
0.20	3.92	89.86	94.7	445.81	0.088
0.35	3.96	89.87	97.7	453.34	0.081
0.40	3.96	89.87	96.8	320.96	0.071
0.45	3.97	89.87	96.1	313.14	0.063
0.60	3.99	89.92	96.8	239.97	0.067
0.80	a = 5.97	90.00	97.9	196.23	0.044
	b = 8.09				
	c = 5.67				

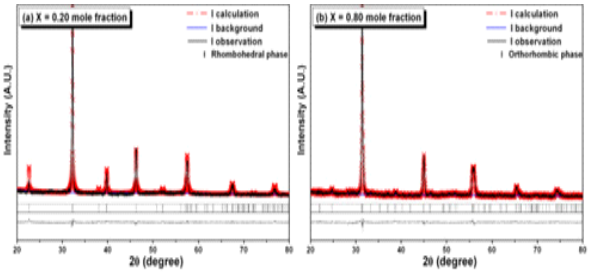

Fig.3. Refinement of BNTZ ceramics. The refinement at (a) 0.20 mole fraction and (b) 0.80 mole fraction showed a rhombohedral phase and an orthorhombic phase, respectively.

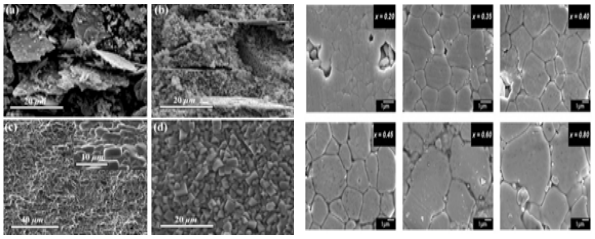

Fig.4. SEM pictures of (a) BNTZ templates, (b) cross section of green samples after binder burnout and (c) cross section surface of sintered textured and $Bi_{0.5}Na_{0.5}Ti_{1-x}Zr_xO_3$ ceramics. Where x = 0.20, 0.35, 0.40, 0.45, 0.60, and 0.80 mole fraction.

In addition, the replacement of larger Zr ions may also cause the dipoles to be poorly induced due to limited ionic movement. This decreasing trend was observed through the sample with a composition of Zr = 0.8, whose structure was orthorhombic. It seemed that the effect of ionic size and limited ionic movement in the perovskite structure of this compound had a greater influence on the dielectric properties than the change in the crystal structure in their unit-all dimentions. Figure 5a, b illustrates the polarization-electric field [PE] hysteresis loops and the breakdown field strengths of BNTZ ceramics, respectively. The hysteresis loops were obtained at the maximum applied electric field of 20 kV/cm and a frequency of 50 Hz. The shape of the P-E loops varied greatly with the ceramic composition. Up to Zr =0.45 mole fraction, the loops showed an ellipse shape due to the vertical deflection electric field with partial dielectric displacement and partly due to conduction. Limited domain reorientation might also be the cause of poor hysteresis loops for these compositions. For samples with Zr = 0.6 and 0.8, the loops showed higher values of remanent polarization though they were still unsaturated.

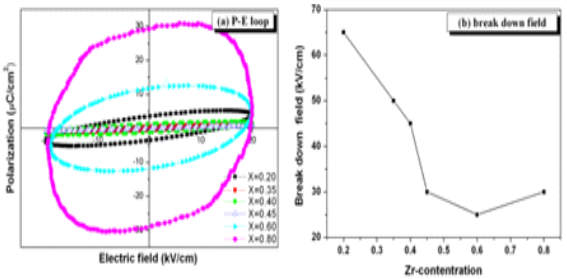

Fig.5. P-E hysteresis loops (a) and the breakdown field (b) of $Bi_{0.5}Na_{0.5}Ti_{1-x}Zr_xO_3$ ceramics. Where x = 0.20, 0.35, 0.40, 0.45, 0.60, and 0.80 mole fraction.

This seemed to show the approximate transition point between the rhombohedral and orthorhombic structures. This was supported by an increase in the breakdown field strength for the Zr = 0.8 composition, which was partly due to the effect of a different crystal structure in this series of materials. Hence, this study showed that the observed dielectric and ferroelectric properties of BNTZ ceramics largely depended on compositional and crystal structure changes. Optimization of these properties could be achieved by fine-tuning the composition for specific applications.

Conclusions

LF- $Bi_{0.5}Na_{0.5}Ti_{1-x}Zr_xO_3$ (where x = 0.20, 0.35, 0.40, 0.45, 0.60, and 0.80 mole fraction) ceramics were successfully fabricated. XRD patterns showed phase transition from rhombohedral to an orthorhombic structure. All ceramic samples were dense with well-defined grain structures. The dielectric constant was found to decrease with increasing Zr content due to the larger sized ionic substitution that limited dipole movement. Ferroelectric properties also showed compositional dependence due to the variation in domain reorientation ability. This study showed that electrical properties of LF-BNTZ ceramics could be further improved by fine-tuning their composition for certain applications.

References

1. Cross LE, Newnham RE: History of ferroelectrics. J Am Ceram 1987, 11:289-305.
2. Haertling GH: Ferroelectric ceramics: history and technology. J Am Ceram 1999, 82:797.
3. Jaffe B, Cook WR, Jaffe H: Piezoelectric Ceramics London: Academic Press; 1971.
4. Kraus W, Nolze G: POWDER CELL- a program for the representation and manipulation of crystal structures and calculation of the resulting X-ray powder patterns. J Appl Cryst 1996, 29:301-303.
5. Lily Kumari K, Prasad K, Yadav KL: Dielectric and impedance study of leadfree ceramic: (Na0.5Bi0.5)ZrO3. J Mater Sci 2007, 42:6252-6259.
6. Moulson AJ, Herbert JM: Electroceramics: Materials, Properties, Applications Chichester: Wiley; 2003.
7. Panda PK: Review: environmental friendly lead-free piezoelectric materials. J Mater Sci 2009, 44:5049-5062.
8. Rachakom et al., Crystal structure and electrical properties of bismuth sodium titanate zirconate ceramics, Nanoscale Research Letters 2012,
9. Shannon RD: Revised effective ionic radii and systematic studies of interatomic distances in halides and chalcogenides. Acta Cryst 1976, A32:751-767.
10. Shrout TR, Zhang SJ: Lead-free piezoelectric ceramics: alternatives for PZT? J Electroceram 2007, 19:111-124.
11. Takenaka T, Nagata H, Hiruma Y, Yoshii Y, Matumono K: Lead-free piezoelectric ceramics based on perovskite structures. 2007, 19:259-265.
12. Tang XG, Chew K-H, Chan HLW: Diffuse phase transition and dielectric tenability of Ba(Zry, Ti1-y)O3 relaxor ferroelectric ceramics. Acta Materialia 2004, 52:5177-5183.
13. Watcharapasorn A, Jiansirisomboon S, Tunkarisi T: Effects of dysprosium oxide addition in bismuth sodium titanate ceramics. J Electroceram 2008, 21:613-616.
14. Watcharapasorn A, Jiansirisomboon S: Dielectric and piezoelectric properties of zirconium-doped bismuth sodium titanate ceramics. Adv Mater Res 2008, 55:133-136.
15. Yu Z, Ang C, Guo R, Bhalla AS: Dielectric properties of Ba(Ti1-xZrx)O3. Mater Lett 2007, 61:326-329.